Fine structure of the Mn acceptor in GaAs

I. V. Krainov,[1,2,*] J. Debus,[3] N. S. Averkiev,[1] G. S. Dimitriev,[1] V. F. Sapega,[1,†] and E. Lähderanta[2]
[1]*Ioffe Institute, Russian Academy of Sciences, 194021 St. Petersburg, Russia*
[2]*Lappeenranta University of Technology, P.O. Box 20, FI-53851, Lappeenranta, Finland*
[3]*Experimentelle Physik 2, Technische Universität Dortmund, 44227 Dortmund, Germany*
(Received 12 April 2016; revised manuscript received 25 May 2016; published 13 June 2016)

We reveal the electronic level structure of the Mn acceptor, which consists of a valence-band hole bound to an Mn^{2+} ion, in presence of applied uniaxial stress and an external magnetic field in bulk GaAs. Resonant spin-flip Raman scattering is used to measure the g factor of the A^0_{Mn} center in the ground and excited states with the total angular momenta $F = 1$ and $F = 2$ and characterize the optical selection rules of the spin-flip transitions between these Mn-acceptor states. We determine the random stress fields near the Mn acceptor, the constant of the antiferromagnetic exchange interaction between the valence-band holes and the electrons of the inner Mn^{2+} shell as well as the deformation potential for the exchange energy. The p-d exchange energy, in particular, decreases significantly with increasing compressive stress. By combining the experimental Raman study with the developed theoretical model on the scattering efficiency, in which also the random local and external uniaxial stresses and magnetic field are considered, the fine structure of the Mn acceptor is determined in full detail.

DOI: 10.1103/PhysRevB.93.235202

I. INTRODUCTION

Diluted magnetic semiconductors (DMSs) offer great potential for efficient spin injection and magnetization manipulation by optical methods so that they are treated nowadays as model materials for the spin electronics [1]. Among the different DMS materials with their promising features, the major attention is drawn on the III-V semiconductor (Ga,Mn)As [2]. A particular feature of the Mn dopant in GaAs is its double role as acceptor providing, at the same time, a hole and magnetic ion to the structure. The hole-mediated interaction between the local magnetic moments of the Mn^{2+} ions leads, as it is commonly accepted, to ferromagnetism in such systems [3].

Recently, it was demonstrated that the magnetization of a thin ferromagnetic (Ga,Mn)As layer can be manipulated by picosecond acoustic pulses [4,5] or by static uniaxial stress [6]. In that context, it was shown that the magnetic anisotropy of (Ga,Mn)As films is controlled by tensile and compressive strains [7,8], which induce an in-plane and out-of-plane orientation of the magnetization, respectively. These observations highlighted that the magnetic anisotropy is caused by mechanical strain occurring in the epitaxial layer. An open question is therefore whether the magnetic anisotropy of (Ga,Mn)As is connected to properties of the individual magnetic Mn acceptors.

The Mn^{2+} impurity in GaAs was investigated by different spectroscopic methods [9–14]. The respective results evidenced that the valence-band hole with total angular momentum $J = 3/2$ is bound to an Mn^{2+} ion whose spin of $S = 5/2$ arises from the $3d^5$ configuration of its inner shell. Magneto-photoluminescence [10] and electron paramagnetic resonance (EPR) [11] studies further demonstrated an antiferromagnetic coupling between the hole and Mn spins. This antiferromagnetic exchange leads, for the complex of the hole bound to an Mn ion, to the formation of four levels that are described by the quantum number $F = J + S = 1,2,3,4$. The effective g factor of the $F = 1$ ground state was determined to $g = 2.77$ and 2.74 by means of EPR [11] and spin-flip Raman scattering (SFRS) [14], respectively. These g factor values are also in good agreement with the Mn-acceptor model developed in Ref. [12]. The ground state is split into two multiplets due to random local stress, while this splitting is smaller than the exchange energy of the Mn acceptor that ranges around 4–6 meV, as evaluated from different indirect studies [12,13]. By directly measuring the energy separation between the $F = 1$ and $F = 2$ states via SFRS the exchange constant was estimated to $\Delta_{F_1\text{-}F_2} = 2.2$ meV that is smaller owing to the nonconsideration of local stress [14,15]. Since the SFRS was successfully used to study exchange interactions and to evaluate exchange constants in DMSs based on II-VI and III-V compounds [14–21], it shall be exploited to study the fine structure of the Mn acceptor in full detail.

In this paper, we determine the electronic structure of the Mn acceptor A^0_{Mn} in bulk GaAs in dependence on uniaxial stress and an external magnetic field. Under uniaxial stress we detect the Raman lines originating from spin-flip transitions between the multiplets of the ground state as well as between the multiplets of the ground and first-excited states and evaluate the corresponding effective g factors. Their dependences on the magnetic field strength and the optical selection rules are discussed. We find that in free bulk GaAs the Mn acceptors experience random local stress, while the exchange energy of the Mn acceptors decreases significantly with the increase of uniaxial compressive stress. Also the effect of the deformation potential on the exchange energy is directly measured. The experimental results are supported by a theoretical model developed for the Mn acceptor in consideration of random local and externally applied uniaxial stresses as well as a magnetic field. This model provides a definite identification of the spin-flip Raman signals and highlights that the previously reported value $\Delta_{F_1\text{-}F_2}$ of the

*igor.kraynov@mail.ru
†sapega.dnm@mail.ioffe.ru

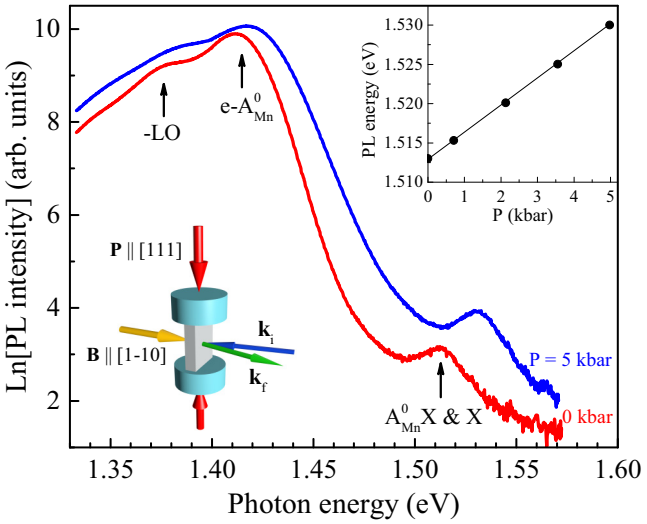

FIG. 1. Band-gap PL spectra of the sample without (red curve) and under application of uniaxial stress (blue curve). Left inset: experimental sketch of the sample (gray cuboid) between two lead plates (blue cylinders). The incident and scattered light vectors are labeled by $\mathbf{k}_i$ and $\mathbf{k}_f$, respectively. Right inset: dependence of the energy position of the merged X and $A^0_{Mn}X$ PL band on the applied stress.

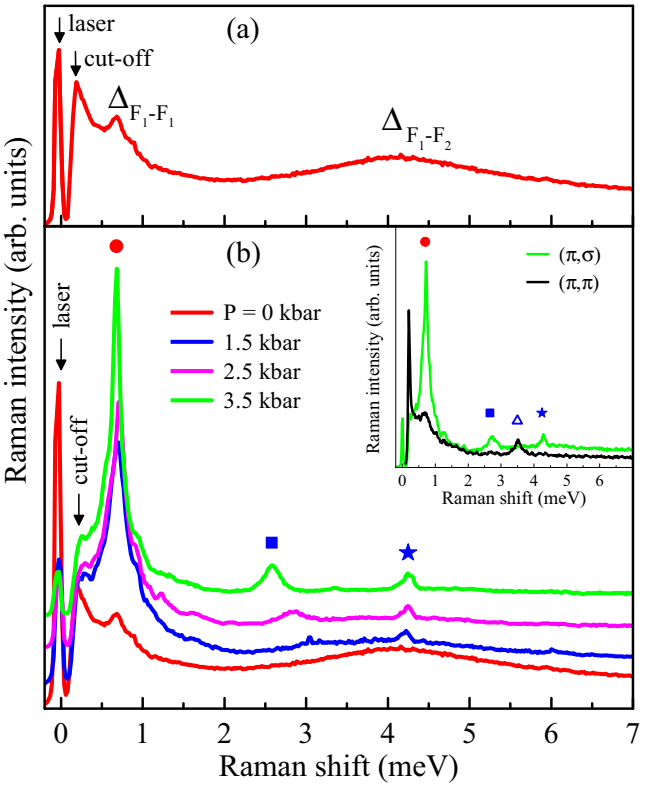

FIG. 2. (a) Raman spectrum of the Mn acceptor obtained in $x(\pi,\sigma)\bar{x}$ configuration at zero magnetic field and in absence of uniaxial stress; $T = 4$ K. Laser line and monochromator cut-off are marked by arrows. (b) Raman spectra of the Mn acceptor in $x(\pi,\sigma)\bar{x}$ geometry for different values of stress applied along the [111] axis; $T = 4$ K, $B = 0$ T. Inset: Raman spectra for the $x(\pi,\sigma)\bar{x}$ (green curve) and $x(\pi,\pi)\bar{x}$ (black curve) geometries; $T = 4$ K, $P = 3.5$ kbar.

hole-Mn-ion exchange energy was underestimated by about 20%.

II. EXPERIMENTAL DETAILS

The bulk GaAs sample was grown in the [111] orientation and with an Mn doping of 6×10^{17} cm^{-3} by the Czochralski process [14]. For the resonant excitation in the SFRS experiments, a tunable Ti:sapphire laser was used. The laser power density on the sample surface was about 5 W/cm^2. An SFRS spectrum was dispersed by a triple-monochromator (DILOR XY) in the subtractive mode and was detected by a charge-coupled device (CCD) camera. The sample was immersed in a continuous He-flow cryostat kept at $T = 4$ K and was exposed to magnetic fields of up to $B = 5$ T which were applied in Faraday geometry along the [1-10] crystal direction. Uniaxial stress of up to $P = 5$ kbar was applied along the [111] direction being perpendicular to the external magnetic field direction, as it is shown in the left inset of Fig. 1.

For describing the circular polarization properties of the SFRS lines, we use the notation $x(\sigma^\eta,\sigma^\lambda)\bar{x}$, where $\bar{x}$ and x are perpendicular to the sample plane and $\eta = \pm,\lambda = \pm$ denote the circular polarization of the exciting σ^η and scattered σ^λ light, respectively. The linear polarization configurations were given by either $x(\pi,\sigma)\bar{x}$ or $x(\pi,\pi)\bar{x}$. In this case the electric field vector of the light is parallel, for π, or perpendicular, for σ, to the [111] axis.

III. RESULTS OF SFRS MEASUREMENTS

The band-gap photoluminescence (PL) spectrum of the externally unstressed GaAs:Mn sample is shown by the red curve in Fig. 1 for $B = 0$ T and $T = 4$ K. The PL band denoted by e-A^0_{Mn}, which is centered at 1.411 eV, arises from the radiative recombination of free and, respectively, localized single electrons (e) with holes bound to neutral Mn acceptors. The longitudinal-optical phonon-assisted PL of the e-A^0_{Mn} band is labeled as -LO in this spectrum. The band at about 1.514 eV has been attributed in Ref. [14] to the overlapping bands of the free exciton (X) and the exciton bound to an Mn acceptor. External uniaxial stress leads to a blueshift of both the e-A^0_{Mn} and the merged X and $A^0_{Mn}X$ bands; see blue curve. The dependence of the excitonic band on the applied stress is shown in the right inset of Fig. 1; its peak energy shifts from $P = 0$ to 5 kbar by about +15 meV.

The Stokes-SFRS spectrum, obtained for resonant excitation of the luminescence band of the excitons bound to neutral Mn acceptors at $E_{exc} = 1.514$ eV, is shown in Fig. 2(a). It contains a sharp asymmetric Raman line, which is shifted by $\Delta_{F_1\text{-}F_1} = 0.7$ meV from the laser line at zero Raman shift, and a broad Raman line at $\Delta_{F_1\text{-}F_2} = 4.4$ meV. The latter one is attributed to the transition within the A^0_{Mn} complex between the $F = 1$ and $F = 2$ states, while the $\Delta_{F_1\text{-}F_1}$ Raman line results from the transition between the states with $m_F = 0$ and $|m_F| = 1$ ($\Delta m_F = \pm 1$) of the acceptor ground state with $F = 1$ that is split due to the local field at the Mn ion site [14]. In order to prove this assignment we study the impact of applied uniaxial stress on the Raman lines. In Fig. 2(b) the

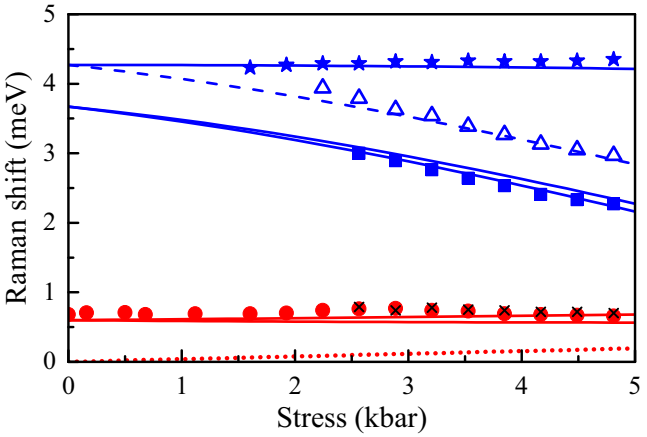

FIG. 3. Shifts of the Raman lines measured in the $x(\pi,\sigma)\bar{x}$ (closed symbols) and $x(\pi,\pi)\bar{x}$ (open triangles) polarization configurations as function of the uniaxial stress along the [111] axis; $T = 4$ K, $B = 0$ T. The experimental error does not exceed the symbol size. The curves are theoretical fits; see details in text.

Raman spectrum (red curve), measured in absence of uniaxial stress, is compared with Raman spectra that are detected for different values of $P > 0$. For each applied stress, the Raman spectrum was measured at resonant excitation of the $A^0_{Mn}X$ band. The $\Delta_{F_1\text{-}F_1}$ Raman line becomes narrower and much more intense with increasing stress. Furthermore, its linear polarization properties are changed: while it is weakly polarized for $P = 0$, it becomes strongly polarized in the stressed sample. The intensity is enhanced in the crossed-linear polarization configuration $x(\pi,\sigma)\bar{x}$, as it is demonstrated in the inset of Fig. 2(b). Moreover, the shift of this Raman line demonstrates a weak, but nonmonotonous dependence on the applied stress; see red solid circles in Fig. 3.

The broad $\Delta_{F_1\text{-}F_2}$ Raman line splits into three narrow lines under application of uniaxial stress; they are marked by symbols in Fig. 2(b) and its inset. Two of these lines (■ and ★) are observed in the crossed $x(\pi,\sigma)\bar{x}$ polarization, while the third (△) is active in the parallel $x(\pi,\pi)\bar{x}$ configuration. The dependence of the Raman shift for each line on the applied stress is depicted in Fig. 3. The Raman lines ■ and △ demonstrate a reduction in their energies with a similar slope for increasing stress, while the Raman line marked by ★ is insensitive to the degree of strain inside the sample. The uniaxial stress splits the $F = 1$ and $F = 2$ states of the Mn acceptor into two ($m_F = 0,\pm1$) and three ($m_F = 0,\pm1,\pm2$) multiplets, respectively. Here, each multiplet is characterized by its angular momentum projection m_F on the stress direction. A magnetic field can remove the twofold degeneracy of a multiplet with nonzero angular momentum projection; accordingly, we apply an external magnetic field to identify the origin of the Raman lines. Figure 4(a) shows circularly polarized Raman spectra measured at $B = 5$ T, for the sample stressed by $P = 4.8$ kbar [22]. One clearly observes several spectrally well-resolved SFRS lines that can be attributed to paramagnetic resonances of the Mn^{2+} impurity and to spin-flip scattering processes within the Mn acceptor.

The Raman shifts of the two lines, marked by ♦ and ◊, vary linearly with the field and tend, for $B = 0$ T, to zero, as it is

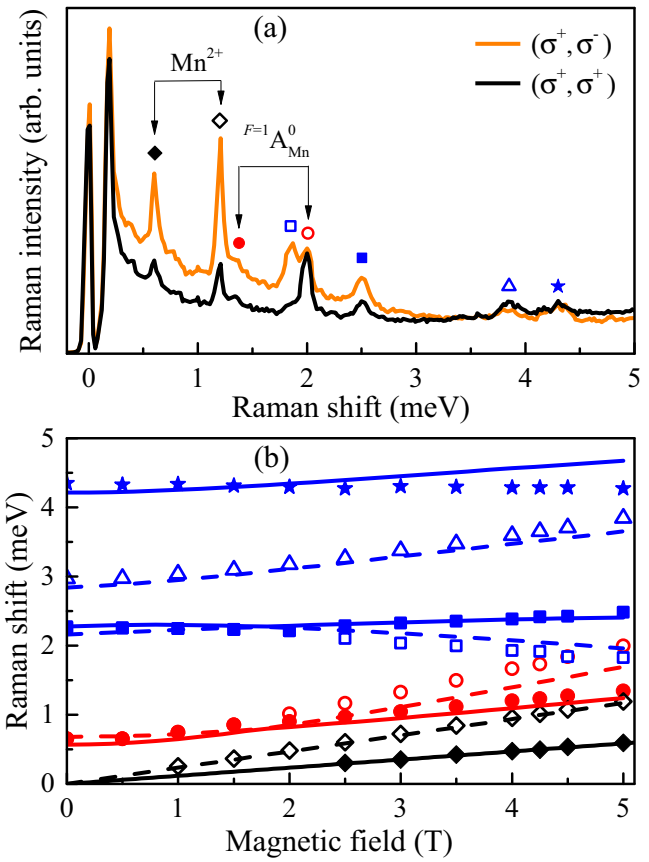

FIG. 4. (a) Raman spectra measured at $B = 5$ T in $x(\sigma^+,\sigma^-)\bar{x}$, orange curve, and $x(\sigma^+,\sigma^+)\bar{x}$, black curve, configurations; $T = 4$ K, $P = 4.8$ kbar. The arrows indicate Raman lines corresponding to transitions between the $F = 1$ states of the Mn acceptor and that of the ionized Mn^{2+} impurity. (b) Magnetic field dependence of the different Raman shifts for $x(\sigma^+,\sigma^-)\bar{x}$, $T = 4$ K, and $P = 4.8$ kbar. Curves are theoretical fits.

illustrated in Fig. 4(b). Their magnetic field dependences can be represented by $E_♦ = g_d\mu_B B$ and $E_◊ = 2g_d\mu_B B$, where μ_B is the Bohr magneton and $g_d = 2.02 \pm 0.02$. Since the g factor value and the polarization characteristics well coincide with that of ionized Mn acceptors [11,14], we conjecture that these low-energetic Raman lines originate from the spin flips of electrons in the inner shell of ionized Mn acceptors.

The Raman lines at 1.38 meV and 2.01 meV are marked by closed and, respectively, open circles in Figs. 4(a) and 4(b). They shift about linearly with increasing B field, which can be described by $E_● = g_{F=1}\mu_B B$ and $E_○ = 2g_{F=1}\mu_B B$ with $g_{F=1} = 2.74 \pm 0.03$. With decreasing magnetic field their Raman shifts approach the same nonzero value $\Delta_{F_1\text{-}F_1}$. These two lines result from transitions between sublevels of the Mn-acceptor ground state $^{F=1}A^0_{Mn}$ split in a magnetic field [11,14].

The SFRS lines that are labeled by the closed square, ★, and △ increase in their energies, while the shift of the Raman line □ decreases with rising magnetic field. The SFRS processes, yielding the lines marked by squares, are dominant in the crossed-circular polarization, the other two do not show any definite polarization features. The origin of these magnetic-

field dependent SFRS lines is not clear and their assignment to transitions between different Zeeman sublevels of the $F = 1$ and $F = 2$ states requires theoretical consideration.

IV. THEORETICAL MODELING

Each of the observed SFRS processes with scattering frequency ω into a solid-angle element $d\Omega$ can be described in terms of the differential scattering intensity $dI/d\omega\, d\Omega \sim |\langle f_{\rm ph} f_{\rm Mn}|\hat{S}|i_{\rm Mn} i_{\rm ph}\rangle|^2$, where $\hat{S}$ is the scattering matrix, I the intensity of the scattered light, and $|i\rangle, |f\rangle$ the initial and final states of the photons (ph) and the Mn acceptor, respectively. The first nonzero contribution to the differential scattering intensity is given by the third order in the perturbation, namely, the second order of the $\hat{V}_{\rm ph}$ electron-photon interaction and the first order of the exchange interaction $\hat{V}_{\rm ex} = A(\hat{\mathbf{S}}\hat{\mathbf{J}})$ between a hole and the $3d^5$ electrons of an Mn ion. Here, the exchange constant is described by A and the operators for the Mn spins and holes are denoted by $\hat{\mathbf{S}}$ and $\hat{\mathbf{J}}$, respectively. The differential intensity of the scattered light can further be presented in the form

$$\frac{dI}{d\omega\, d\Omega} \sim |\langle f_{\rm Mn}|(2\hat{S}_z a_z + \hat{S}_- a_+ + \hat{S}_+ a_-)|i_{\rm Mn}\rangle|^2, \quad (1)$$

$$\mathbf{a} \sim \langle f_{\rm ph}|(\hat{\mathbf{e}}\hat{\mathbf{p}})\hat{\mathbf{J}}(\hat{\mathbf{e}}\hat{\mathbf{p}})|i_{\rm ph}\rangle, \quad (2)$$

where $\hat{\mathbf{e}}$ is the electric field operator and $\hat{\mathbf{p}}$ the electron momentum operator. The vector $\mathbf{a}$ determines the polarization properties of the scattered light. For the $x(\pi,\sigma)\bar{x}$ configuration, $a_z = 0$ and $a_\pm \sim 1$, while, for the copolarized $x(\pi,\pi)\bar{x}$ configuration, $\mathbf{a} = 0$. However, in the fourth-order perturbation a double spin-flip process is allowed in the $x(\pi,\pi)\bar{x}$ configuration, and it is related to the components $(\hat{S}_+\hat{J}_-)(\hat{S}_-\hat{J}_+)$ or $(\hat{S}_+\hat{J}_-)(\hat{S}_+\hat{J}_-)$ of the scattering matrix. In exact Faraday geometry, for the $x(\sigma^+,\sigma^-)\bar{x}$ polarization configuration, $\mathbf{a}$ vanishes in the third-order perturbation, and only in fourth-order perturbation a double spin-flip process corresponding to $(\hat{S}_+\hat{J}_-)(\hat{S}_+\hat{J}_-)$ becomes allowed. However, a tilting of the incident beam by 10°–15° out of the normal of the sample plane activates the SFRS process in the crossed $x(\sigma^+,\sigma^-)\bar{x}$ polarization, which is the same as for the $x(\pi,\sigma)\bar{x}$ and $x(\pi,\pi)\bar{x}$ configurations.

To calculate the SFRS signal one has to use the Mn spin operator in the interaction representation $\hat{\mathbf{S}}(t) = e^{i\hat{H}_0 t}\hat{\mathbf{S}}e^{-i\hat{H}_0 t}$, where $\hat{H}_0$ is the effective Hamiltonian of the Mn acceptor that will be described in the following. Accordingly, $\langle f_{\rm Mn}|\hat{\mathbf{S}}(t)|i_{\rm Mn}\rangle$ can be written as $e^{i\Delta t}\langle f_{\rm Mn}|\hat{\mathbf{S}}|i_{\rm Mn}\rangle$ with the difference between the eigenvalues of $\hat{H}_0$ given by $\Delta = \omega_{f_{\rm Mn}} - \omega_{i_{\rm Mn}}$, which defines the Raman shift. The effective Hamiltonian, which specifies the interaction between the Mn^{2+} ion and localized hole (h) in the $A^0_{\rm Mn}$ complex, can be formulated by

$$\hat{H}_0 = \hat{H}_{\rm loc} + A(\hat{\mathbf{S}}\hat{\mathbf{J}}) + \mu_{\rm B} g_{\rm d}(\hat{\mathbf{S}}\mathbf{B}) - \mu_{\rm B} g_{\rm h}(\hat{\mathbf{J}}\mathbf{B}) - b\sum_i \epsilon_{ii}\hat{J}_i^2 - d\sum_{ij}\epsilon_{ij}\{\hat{J}_i\hat{J}_j\} + \delta\sum_{ij} n_i n_j \{\hat{J}_i\hat{J}_j\}. \quad (3)$$

$\hat{H}_{\rm loc}$ describes the localization of the Mn acceptor, ϵ_{ij} is the strain tensor, b,d are the deformation potentials of the Mn acceptor, δ represents the fluctuation field strength, n denotes the direction cosine of the fluctuation field, and the rule $\{\hat{J}_i\hat{J}_j\} = (\hat{J}_i\hat{J}_j + \hat{J}_j\hat{J}_i)/2$ applies, where i,j stands for one of the directions x,y, and z. Fluctuation fields acting on the Mn-hole complex in some point of space shall be presented in the form $\delta\hat{J}^2_{z'}$ with the random direction z'. The fluctuation fields can be caused by the presence of random local strain and/or Mn^{2+} charged centers [3].

The directly measured exchange constant $\Delta_{\rm F_1\text{-}F_2}$, which is about 2.2 meV [14], exceeds the stress energies bP/C_{ii} and dP/C_{ii} as well as Zeeman energies, where C_{ii} stands for the elastic constants of GaAs. By considering the exchange interaction, the energetically degenerate levels of the Mn acceptor (total number is 24) are split into four levels, which are characterized by the total angular momenta $F = S + J = 1,2,3,4$ with a degree of degeneracy of $2F + 1$. A further splitting of these four levels is caused by strain, fluctuation fields, and an external magnetic field. The effective Hamiltonians, which describe the effects of the deformations and the magnetic field on the $F = 1$ ground and first-exited $F = 2$ states, are expressed by

$$\hat{H}_{F=1} = \mu_{\rm B}\left(\frac{7}{4}g_{\rm d} + \frac{3}{4}g_{\rm h}\right)(\hat{\mathbf{F}}\mathbf{B}) - \frac{21}{20}[b{\rm Sp}(\hat{\epsilon}) + \delta]\hat{I} - \frac{3}{10}b\sum_i \hat{F}_i^2\epsilon_{ii} - \frac{3}{10}d\sum_{ij}\{\hat{F}_i\hat{F}_j\}\epsilon_{ij} + \frac{3}{10}\delta\sum_{ij}\{\hat{F}_i\hat{F}_j\}n_i n_j, \quad (4)$$

$$\hat{H}_{F=2} = \mu_{\rm B}\left(\frac{11}{12}g_{\rm d} - \frac{1}{12}g_{\rm h}\right)(\hat{\mathbf{F}}\mathbf{B}) + \left[2A - \frac{55}{28}b{\rm Sp}(\hat{\epsilon}) - \frac{55}{28}\delta\right]\hat{I} + \frac{5}{14}b\sum_i \hat{F}_i^2\epsilon_{ii} + \frac{5}{14}d\sum_{ij}\{\hat{F}_i\hat{F}_j\}\epsilon_{ij} - \frac{5}{14}\delta\sum_{ij}\{\hat{F}_i\hat{F}_j\}n_i n_j + 2A_P{\rm Sp}(\hat{\epsilon})\hat{I}. \quad (5)$$

Both Hamiltonians contain the identity matrix $\hat{I}$ and angular momentum operator $\hat{\mathbf{F}}$ with corresponding dimensionality. The stress-dependent exchange energy for the $F = 2$ multiplet is given by the fit parameter A_P in Eq. (5). By using the Hamiltonians (4) and (5) we calculate the energy levels of the Mn acceptor in magnetic, random, and uniaxial stress fields. It is worthwhile to mention that taking into account random local fields, which act on the Mn acceptor, requires, for the calculation of the SFRS transitions, the averaging over all possible orientations z' of the random fields.

V. DISCUSSION AND CONCLUSION

In this section we compare the data of the SFRS measurements with the aforedescribed theoretical model of the Mn-acceptor fine structure in the presence of a random local field, external uniaxial stresses, and a magnetic field. For the calculations, the following parameters are used: $g_{\rm d} = 2.02$ [13,14,23], $g_{\rm h} = -1$ [19,23], $d = 3.1$ eV [13], $\delta = 2$ meV [12], and the elastic constants $C_{11} = 12.2$ kbar, $C_{12} = 5.5$ kbar,

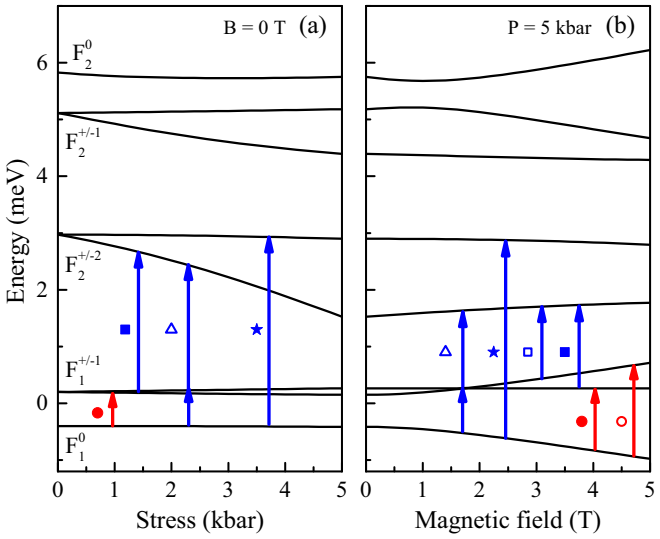

FIG. 5. Calculated level energies of the $F = 1$ and $F = 2$ multiplets with random strain $\delta = 2$ meV oriented along the [001] axis. Dependence of the Mn-acceptor level energies on (a) uniaxial stress that is parallel to the [111] axis and on (b) a magnetic field along the [1-10] axis. Vertical arrows marked by symbols correspond to the experimentally observed SFRS transitions between Mn-acceptor multiplets with $F = 1$ and $F = 2$, see text for details.

and $C_{44} = 6.2$ kbar taken from Ref. [24]. From the theoretical simulations of the experimental data we further evaluate the p-d exchange constant to $A = 2.6$ meV ($> \Delta_{F_1\text{-}F_2}$) and the stress-dependent exchange energy to $A_P = 0.9$ eV.

The calculated energies of the Mn-acceptor ground and first-excited states as a function of the uniaxial stress is shown in Fig. 5(a). Here, we consider that in absence of external stress ($P = 0$) the Mn acceptor experiences random local stress that shall now be directed, for simplicity, along the [001] axis. This random stress leads to a splitting of the ground and first-excited states into $F_1^0, F_1^{\pm 1}$ and $F_2^0, F_2^{\pm 1}$, $F_2^{\pm 2}$ multiplets, respectively. Here, the lower index denotes the total angular momentum and the upper index its projection m_F onto the [001] axis, which is a good quantum number in the absence of external fields. Note that the degeneracy of the energetically lowest multiplet is determined by the sign of the random stress δ. The uniaxial stress applied along the [111] direction gives rise to a further splitting of the $F = 1$ and $F = 2$ multiplets. Besides this dependence of the ground and first-exited states on the external stress, we demonstrate in Fig. 5(b) the magnetic field behavior of the Mn-acceptor multiplets, whereby the external uniaxial stress is set to $P = 5$ kbar. The red arrows in Figs. 5(a) and 5(b) show transitions between the multiplets characterized by the total angular momentum $F = 1$. These transitions correspond to SFRS lines whose dependences on the external stress and magnetic field are shown by circles in Figs. 3, 4(a), and 4(b). In these figures, the theoretical fits of the stress and magnetic field dependences of the SFRS transitions are, for comparison, depicted by curves.

It is seen that uniaxial stress applied along the [111] direction does not change noticeably the initial splitting induced by random stress. This theoretical prediction is in good agreement with the experimental observation. In the model, in which the absence of fluctuating random stress is assumed, the splitting of the $F = 1$ state due to external uniaxial stress shows a weak linear dependence, as it is demonstrated by the dotted line in Fig. 3. Under magnetic field application the ground state splits into three Zeeman sublevels. The calculated g factor of these states with $F = 1$ amounts to $g \sim 2.75$ coinciding with the measured value $g = 2.74$; see also circles in Fig. 4. It is worth to mention that pronounced SFRS lines appear, for $B > 0$, when the Zeeman energy is comparable with the random splitting. This is a direct evidence for the positive sign of the random stress, and it is also in line with the prediction given in Ref. [12]. The value of the $F = 1$ state splitting induced by the random stress δ directly corresponds to the Raman shift (0.6–0.7 meV) of the $\Delta_{F_1\text{-}F_1}$ Raman line at zero uniaxial stress.

Let us discuss now the SFRS lines related to interlevel transitions, i.e., transitions between the states of the multiplets with $F = 1$ and $F = 2$. The transitions that are active in the SFRS processes are indicated by blue arrows in Fig. 5. Transitions to the $F = 2$ states shall take place from the lowest multiplets F_1^0 and $F_1^{\pm 1}$ because both can be assumed to be populated. This assumption is justified by the fact that the relation $(E_{\pm 1}^{F=1} - E_0^{F=1})/(k_B T) \approx 1$ is fulfilled in the experiments; k_B is the Boltzmann constant. The polarization properties of the SFRS lines allow one to assign them to particular interlevel transitions: according to the selection rules for the SFRS processes discussed in the frame of Eqs. (1) and (2), transitions, in which the Mn and hole spin is changed each by $|1|$, are present in the Raman spectra in crossed-polarized configurations. Therefore, the Raman lines that are observed in the $x(\pi,\sigma)\bar{x}$ polarization can be assigned to transitions between the $F = 1$ and $F = 2$ multiplet states, for ■, and from F_1^0 to the $F = 2$ multiplet, for ★. The same selection rules govern the Raman process involving a double spin-flip in the copolarized $x(\pi,\pi)\bar{x}$ configuration. Hence, the Raman line marked by the open triangle consists (i) of the transition between the multiplets of the ground state and, afterwards, (ii) of the scattering process to the $F = 2$ multiplet. This double spin-flip process is shown schematically by a sequence of two arrows in Fig. 5. In accord with this diagram, the energy difference between the transitions belonging to the ■ and △ lines exactly coincides with the energy of the transition between the states with $F = 1$; see red arrow in Fig. 5(a) as well as the crosses in Fig. 3.

We propose that the double spin-flip process takes place in an individual Mn acceptor. This assumption is supported by the fact that in the sample studied ($N_{Mn} \sim 6 \times 10^{17}$ cm^{-3}) the distance between neighboring Mn ions is similar to the exciton Bohr radius ($N_{Mn} a_B^3 \sim 1$). Hence, this comparably large distance prevents the realization of a double spin-flip process from sequential spin excitations in two neighboring Mn acceptors. Moreover, the charge compensation of the Mn acceptors, which is clearly demonstrated by the observation of the d-shell related Mn^{2+} SFRS line, makes double spin-flip processes involving neighboring Mn acceptors improbable. A partial compensation could be due to interstitial Mn double donors [25]. Note that multiple spin-flip processes involving neighboring Mn acceptors become important with increasing Mn concentration, as it was shown in Ref. [14] for Mn^{2+} ions.

In an external magnetic field, SFRS processes based on transitions between Zeeman sublevels with $F = 2$ are not observed due to their negligible population at the low temperature measured. Nevertheless, scattering processes between Zeeman sublevels with $F = 1$ and $F = 2$ are detected; they are indicated by the blue color in the panels of Figs. 3, 4, and 5. The magnetic field dependence of these lines allows for estimating the g factor of the $F = 2$ multiplet to $g = 23/12$ based on fits according to Eq. (5) and the consideration of $g = 2.74$ for the $F = 1$ multiplet.

Let us finally discuss the effect of uniaxial stress on the p-d exchange constant A. In a strain-free material the exchange constant is given by half of the energy separation between the $F = 1$ and $F = 2$ states. In our model, the uniaxial stress applied along the [111] direction does not change the relative energy distance between these states, while the experimental data clearly show the decrease in their energy separation. This decrease cannot be explained either with the deformation potential for the Mn acceptor or with, e.g., a twice larger d value given by [26] 5–6 eV. We conjecture that the reduction in the relative energy separation between the $F = 1$ and $F = 2$ multiplets is caused by the stress dependence of the exchange interaction between the inner d shell of the Mn ion and the valence-band hole. To take into account the impact of uniaxial stress on the exchange constant A one needs to calculate the stress-dependent overlap integral of the carrier-wave functions [27,28]. The dependence of stress on A can be described phenomenologically by expanding the exchange constant in powers of the external stress P. In the first-order approximation one can write

$$A(\hat{\epsilon}) = A + A_P \mathrm{Sp}(\hat{\epsilon}).$$

This approximation leads to Eqs. (4) and (5). From the fits to the stress dependences of the Raman shifts, where the excited $F = 2$ states are involved, see blue-colored curves in Fig. 3, we estimate the value of $A_P = 0.9$ eV. This means that the p-d exchange constant decreases by about $\Delta A(P)/A(0) \approx 20\%$ for uniaxial compressive stress of $P = 5$ kbar, which is approximately half of the destructive stress (11 kbar) directed along the [111] axis.

In conclusion, we characterize the fine structure of the Mn acceptor in bulk GaAs, for the multiplets with the total angular momenta $F = 1$ and $F = 2$, in the presence of uniaxial stress and an external magnetic field by using resonant spin-flip Raman scattering. We demonstrate that even without external stress the Mn acceptor experiences random local stress that induces a splitting of the ground $F = 1$ state of up to 0.7 meV. It is also shown that uniaxial compressive stress leads surprisingly to a significant reduction of the p-d exchange interaction strength and to a deformation potential value of the exchange constant given by $A_P = 0.9$ eV. Furthermore, the measured effective g factor of the excited $F = 2$ states is comparable with the theoretically predicted $g = 23/12$ value. The developed theoretical model of the Mn acceptor, which considers random local and external uniaxial stresses as well as a magnetic field, satisfactorily describes the observed spin-flip Raman lines and their polarization characteristics. Our study on the spin-flip Raman scattering of the Mn acceptors in GaAs underlines that their individual properties are essential to explain the stress dependence of the antiferromagnetic hole-Mn exchange interaction. These results may be considered as a step toward understanding the magnetic anisotropy of (Ga,Mn)As as a result of the individual Mn acceptors and may be employed for other acceptor complexes in III-V semiconductor structures.

ACKNOWLEDGMENTS

Theoretical calculations were performed within the project of Russian Science Foundation No. 14-12-00255 (I.V.K. and N.S.A.); the experimental part of the work was supported by the Russian Foundation for Basic Research, Grant No. 15-52-12017 NNIO-a, and Russian Ministry of Education and Science, Contract No. 14.Z50.31.0021 (V.F.S. and G.S.D.). J.D. acknowledges support from the Deutsche Forschungsgemeinschaft in the framework of the ICRC TRR 160.

[1] *Introduction to the Physics of Diluted Magnetic Semiconductors*, edited by J. Kossut and J. A. Gaj (Springer, Heidelberg, 2010).
[2] T. Dietl and H. Ohno, Rev. Mod. Phys. **86**, 187 (2014).
[3] T. Jungwirth, J. Sinova, J. Mašek, J. Kučera, and A. H. MacDonald, Rev. Mod. Phys. **78**, 809 (2006).
[4] A. V. Scherbakov, A. S. Salasyuk, A. V. Akimov, X. Liu, M. Bombeck, C. Brüggemann, D. R. Yakovlev, V. F. Sapega, J. K. Furdyna, and M. Bayer, Phys. Rev. Lett. **105**, 117204 (2010).
[5] M. Bombeck, A. S. Salasyuk, B. A. Glavin, A. V. Scherbakov, C. Brüggemann, D. R. Yakovlev, V. F. Sapega, X. Liu, J. K. Furdyna, A. V. Akimov, and M. Bayer, Phys. Rev. B **85**, 195324 (2012).
[6] V. F. Sapega, I. V. Kraynov, N. I. Sablina, G. S. Dimitriev, N. S. Averkiev, and K. H. Ploog, Solid State Commun. **157**, 34 (2013).
[7] A. Shen, H. Ohno, F. Matsukura, Y. Sugawara, N. Akiba, T. Kuroiwa, A. Oiwa, A. Endo, S. Katsumoto, and Y. Iye, J. Cryst. Growth **175-176**, 1069 (1997).
[8] U. Welp, V. K. Vlasko-Vlasov, X. Liu, J. K. Furdyna, and T. Wojtowicz, Phys. Rev. Lett. **90**, 167206 (2003).
[9] W. Schairer and M. Schmidt, Phys. Rev. B **10**, 2501 (1974).
[10] I. Ya. Karlik, I. A. Merkulov, D. N. Mirlin, L. P. Nikitin, V. I. Perel, and V. F. Sapega, Fiz. Tverd. Tela **24**, 3550 (1982) [Sov. Phys. - Solid State **24**, 2022 (1982)].
[11] J. Schneider, U. Kaufmann, W. Wilkening, M. Baeumler, and F. Köhl, Phys. Rev. Lett. **59**, 240 (1987).
[12] N. S. Averkiev, A. A. Gutkin, E. B. Osipov, and M. A. Reshchikov, Fiz. Tverd. Tela **30**, 765 (1988) [Sov. Phys. - Solid State **30**, 438 (1988)].
[13] M. Linnarsson, E. Janzén, B. Monemar, M. Kleverman, and A. Thilderkvist, Phys. Rev. B **55**, 6938 (1997).
[14] V. F. Sapega, T. Ruf, and M. Cardona, Phys. Status Solidi B **226**, 339 (2001).
[15] V. F. Sapega, M. Moreno, M. Ramsteiner, L. Däweritz, and K. Ploog, Phys. Rev. B **66**, 075217 (2002).
[16] A. Petrou, D. L. Peterson, S. Venugopalan, R. R. Galazka, A. K. Ramdas, and S. Rodriguez, Phys. Rev. Lett. **48**, 1036 (1982).

[17] D. L. Peterson, D. U. Bartholomew, U. Debska, A. K. Ramdas, and S. Rodriguez, Phys. Rev. B **32**, 323 (1985).
[18] A. Petrou, D. L. Peterson, S. Venugopalan, R. R. Galazka, A. K. Ramdas, and S. Rodriguez, Phys. Rev. B **27**, 3471 (1983).
[19] I. V. Krainov, V. F. Sapega, N. S. Averkiev, G. S. Dimitriev, K. H. Ploog, and E. Lähderanta, Phys. Rev. B **92**, 245201 (2015).
[20] J. Debus, D. Dunker, V. F. Sapega, D. R. Yakovlev, G. Karczewski, T. Wojtowicz, J. Kossut, and M. Bayer, Phys. Rev. B **87**, 205316 (2013).
[21] J. Debus, V. F. Sapega, D. Dunker, D. R. Yakovlev, D. Reuter, A. D. Wieck, and M. Bayer, Phys. Rev. B **90**, 235404 (2014).
[22] The energy shift of the excitonic PL band under application of a magnetic field is negligibly small; therefore, the excitation energy was set to the exciton resonance only when the external stress was changed.
[23] V. F. Sapega, N. I. Sablina, I. E. Panaiotti, N. S. Averkiev, and K. H. Ploog, Phys. Rev. B **80**, 041202 (2009).
[24] Yu. A. Burenkov, Yu. M. Burdukov, S. Yu. Davidov, and S. P. Nikanorov, Fiz. Tverd. Tela **15**, 1757 (1973) [Sov. Phys. - Solid State **15**, 1175 (1973)].
[25] K. M. Yu, W. Walukiewicz, T. Wojtowicz, I. Kuryliszyn, X. Liu, Y. Sasaki, and J. K. Furdyna, Phys. Rev. B **65**, 201303 (2002).
[26] N. S. Averkiev, A. A. Gudkin, N. M. Kolchanova, and M. A. Reshikov, Fiz. Techn. Poluprovodn. **18**, 1629 (1984) [Sov. Phys. - Semicond. **18**, 1019 (1984)].
[27] A. M. Monakhov, N. I. Sablina, N. S. Averkiev, C. Çelebi, and P. M. Koenraad, Solid State Commun. **146**, 416 (2008).
[28] A. M. Yakunin, A. Y. Silov, P. M. Koenraad, J.-M. Tang, M. E. Flatte, J.-L. Primus, W. Van Roy, J. De Boeck, A. M. Monakhov, K. S. Romanov, I. E. Panaiotti, and N. S. Averkiev, Nat. Mater. **6**, 512 (2007).